Available online at www.sciencedirect.com
ScienceDirect
Icarus 186 (2007) 581–584
ICARUS
www.elsevier.com/locate/icarus

Note

Arecibo radar observations of Phobos and Deimos

Michael W. Busch [a,*], Steven J. Ostro [b], Lance A.M. Benner [b], Jon D. Giorgini [b], Christopher Magri [c], Ellen S. Howell [d], Michael C. Nolan [d], Alice A. Hine [d], Donald B. Campbell [e], Irwin I. Shapiro [f], John F. Chandler [f]

[a] *Division of Geological and Planetary Sciences, California Institute of Technology, MC 150-21, Pasadena, CA 91125, USA*
[b] *Jet Propulsion Laboratory, California Institute of Technology, Pasadena, CA 91109-8099, USA*
[c] *University of Maine at Farmington, Preble Hall, 173 High St., Farmington, ME 04938, USA*
[d] *Arecibo Observatory, National Astronomy and Ionosphere Center, HC03 Box 53995, Arecibo, PR 00612, USA*
[e] *Department of Astronomy, Space Sciences Building, Cornell University, Ithaca, NY 14853, USA*
[f] *Harvard-Smithsonian Center for Astrophysics, 60 Garden St., Cambridge, MA 02138, USA*

Received 20 September 2006; revised 3 November 2006

Available online 14 December 2006

Abstract

In November 2005, we observed the moons of Mars using the Arecibo 2380-MHz (13-cm) radar, obtaining a result for the OC radar albedo of Phobos (0.056 ± 0.014) consistent with its previously reported radar albedo and implying an upper bound on its near-surface bulk density of 1.6 ± 0.3 g cm^{-3}. We detected Deimos by radar for the first time, finding its OC radar albedo to be 0.021 ± 0.006, implying an upper bound on its near-surface density of 1.1 ± 0.3 g cm^{-3}, consistent with a high-porosity regolith. We briefly discuss reasons for these low radar albedos, Deimos' being possibly the lowest of any Solar System body yet observed by radar.

Keywords: Mars, satellites; Radar observations; Regoliths

1. Observations

The martian satellites were first observed by radar in 1988, when Ostro et al. (1989) detected Phobos using the Goldstone 8510-MHz (3.5-cm) system. They estimated the radar albedo (defined as the radar cross-section in a specified polarization divided by the target's projected area) using an ellipsoidal model for Phobos' shape. However, that crude model's projected areas are ∼15% smaller than those of the very detailed shape model subsequently derived from Mariner 9 and Viking stereo images (Thomas, 1993) and later re-calibration of the Goldstone antenna indicated that the gain was a factor of 1.62 ± 0.02 higher than estimated in 1988, so the cross-section estimate must be adjusted accordingly. Applying these corrections, Ostro et al.'s value for Phobos' mean OC (opposite-sense circular polarization to that transmitted) radar albedo is 0.049 ± 0.012.

We attempted to observe Phobos and Deimos during the 1988 and 1990 Mars oppositions with the Arecibo 2380-MHz (12.6-cm) radar, before its mid-1990s upgrade, obtaining weak Phobos echoes and an OC albedo consistent with the Goldstone result (Fig. 1a, Table 1). Deimos, which is much smaller than Phobos (effective radius ∼6 km versus ∼11 km), eluded detection, but our observations set a three-sigma upper bound of 0.04 on the OC albedo.

On November 2, 2005, we observed both objects with the upgraded Arecibo telescope, which is much more sensitive than Goldstone's 70-m DSS-14 antenna. This advantage was partially offset by scheduling pressure from Mars radar observations, which left only a single track available for observing the satellites. We devoted the first transmit-receive cycle ("run") to Phobos, saw an echo immediately in the real-time display, and allocated the rest of the track (8 runs) to Deimos.

In a radar experiment, to avoid smearing of accumulated echoes in frequency, one tunes the receiver or the transmitter according to a Doppler-prediction ephemeris. Our 2005 observations used Phobos and Deimos ephemerides based on the MAR033 solution of Jacobson (1996). However, upon reducing the data, we noted that our Deimos power spectrum was ∼16 Hz wider than the echo bandwidth of 13.6 Hz predicted from Deimos' known spin period, dimensions, and orientation during the observations. That is, our ephemeris' inaccuracy had allowed Doppler drift in the echo over the course of our integration. Therefore, we re-reduced the data using a much more accurate ephemeris (MAR063; Jacobson and Rush, 2006), which became available in April 2006. The result was a summed-spectrum bandwidth of 14 ± 2 Hz. For Phobos, the frequency drift due to use of MAR033 was about 2 Hz, smaller than our 5-Hz spectral resolution and very small compared to Phobos' ∼100 Hz bandwidth. Since the drift can have no effect on the results reported here and would be imperceptible in Fig. 1, we did not re-reduce the Phobos data.

Our Phobos run yielded an OC radar albedo of 0.056 ± 0.014 (Fig. 1b, Table 1), in agreement with the 1988 and 1990 results. Summing the eight Deimos runs (Fig. 1c), we find an OC radar cross-section of 2.9 ± 0.8 km^2, correspond-

* Corresponding author.
E-mail address: busch@caltech.edu (M.W. Busch).

0019-1035/$ – see front matter
doi:10.1016/j.icarus.2006.11.003

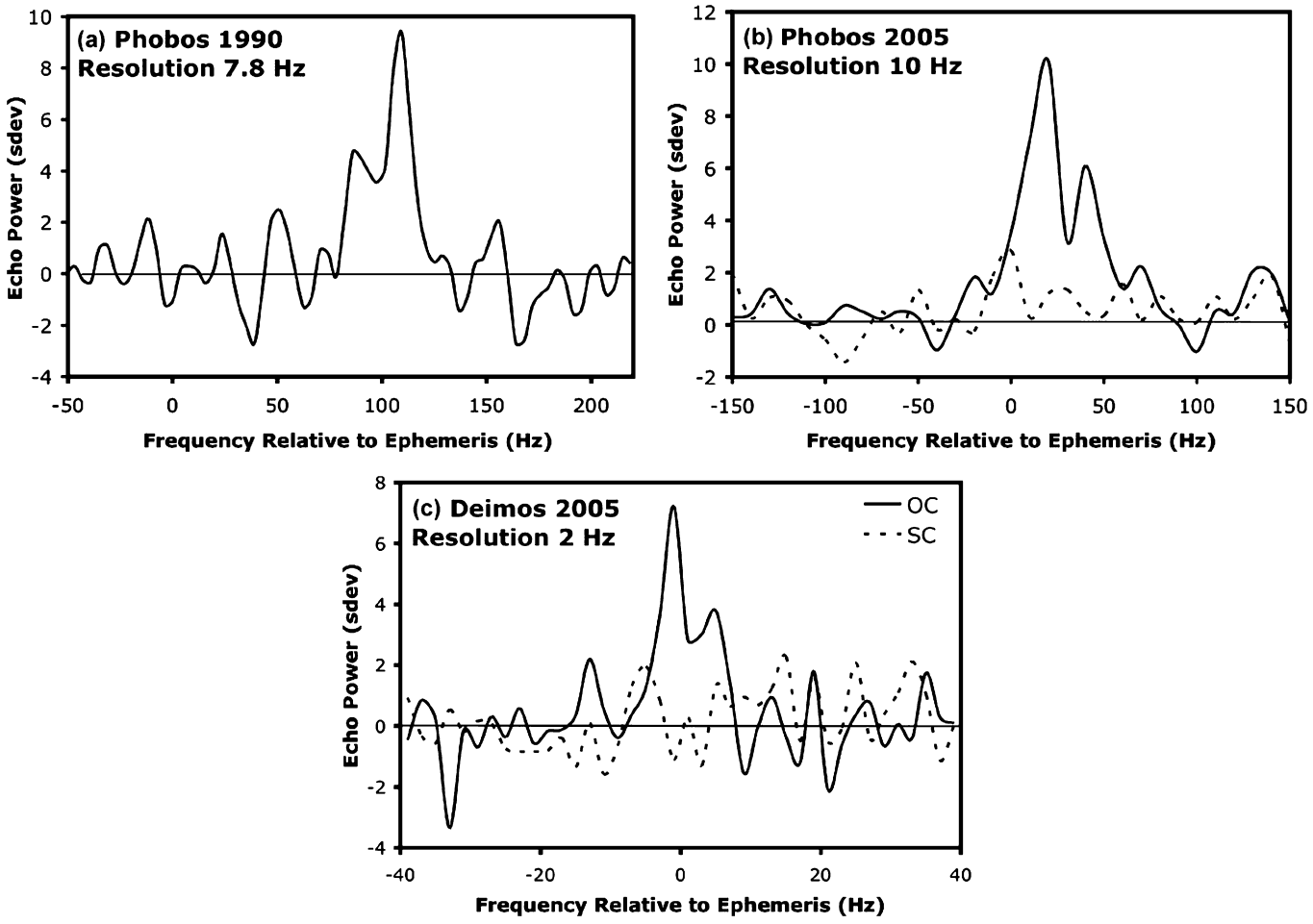

Fig. 1. Echo power spectra. (a) Phobos from 1990, (b) Phobos from 2005, and (c) Deimos from 2005. The 1990 spectrum is the best single-day detection in that year (Table 1). The frequency resolution has been smoothed from a raw value of 3.9 to 7.8 Hz in (a), from 5.0 to 10 Hz in (b), and from 0.2 to 2.0 Hz in (c). Echo strength is plotted in standard deviations. The Phobos Doppler prediction ephemerides used an approximate analytical theory for the motion of this moon; the observed offsets are not dynamically significant and have no bearing on the results in this paper.

Table 1
Observations and disc-integrated results

Target	Phobos	Phobos	Deimos
Observation epoch	1990 Nov 12	2005 Nov 2	2005 Nov 2
(UTC)	04:58:34–05:52:41	03:40:09–03:47:45	03:59:35–05:55:34
Runs	13	1	8
Rotation phase coverage (°)	42	6	23
T_{sys} (K)	48	25	25
Gain (dB)	141	147	146
Transmitter power (kW)	415	434	434
Subradar latitude and longitude (°)	(−13, 345)	(−28, 273)	(−28, 91)
Projected area (km^2)	362 ± 4	407 ± 5	137 ± 4
OC cross-section (km^2)	22.9 ± 6.4	22.8 ± 6.6	2.9 ± 0.8
SC/OC cross-section ratio	–	0.17 ± 0.04	0.12 ± 0.12
OC radar albedo	0.064 ± 0.014	0.056 ± 0.014	0.021 ± 0.006

Note. For each observation we give the number of transmit-receive cycles ("runs"), the rotation phase coverage, the system noise temperature, the two-way gain of the Arecibo telescope, and the target's average subradar latitude, subradar longitude, and projected area. The 1990 data are for the spectrum shown in Fig. 1. Projected areas are from the models of Thomas (1993). We do not have SC data from the 1990 observations.

ing to an OC albedo of 0.021 ± 0.006, again based on a shape model derived from stereo images (Thomas, 1993).

The Arecibo receivers detect both SC (same-sense circular polarization as transmitted) and OC echoes simultaneously. We estimate circular polarization echo power ratios, SC/OC, of 0.17 ± 0.04 for Phobos and 0.12 ± 0.12 for Deimos.

The disc-integrated radar properties of Mars' moons are unusual compared to available values for other small bodies (Benner, 2006). Phobos has a radar albedo near the low end of the distribution for radar-observed asteroids, while Deimos seems to have the lowest radar albedo of any radar-detected Solar System object. Both moons have lower polarization ratios than almost all radar-observed comets. Since SC/OC measures near-surface structural complexity on

cm-to-m scales while radar albedo is primarily sensitive to bulk density, we conclude that the moons' surfaces are relatively low-density and smooth.

2. Near-surface bulk densities

For a smooth sphere, the OC radar albedo would equal R, the Fresnel normal-incidence reflectance coefficient, and SC/OC would be zero. For a target that has decimeter-scale 'roughness' within a meter or so of the surface, some of the echo power is converted into SC via single scattering from rough surfaces or via multiple scattering. Some fraction of the OC radar albedo then corresponds to R for a hypothetical smooth component of the surface.

One can write $R = \text{OC albedo}/g$ for non-spherical rough objects, where the backscatter gain g is greater than 1. R for a homogenous dielectric half-space with a perfectly smooth boundary is an increasing function of the bulk density d. If we assume $g = 1$, we set an upper bound on R, and therefore an upper bound on the bulk density of the smooth component of the near-surface. The martian satellites' low SC/OC ratios indicate that single back-reflections dominate the echoes. Since a small fraction of the OC echoes is likely due to scattering other than single back-reflections, our upper bounds on R are conservative.

Several approximate $d(R)$ formulas for real materials have been derived from empirical results, either by using the radar albedos of asteroids visited by spacecraft or by measuring the radar reflectivity of laboratory powders. Magri et al. (2001) used the surface density of 433 Eros as determined from the NEAR spacecraft to calibrate their $d(R)$ relationship. Ostro et al. (1985) and Garvin et al. (1985) measured R for powders of various densities and compositions and found a nearly linear or logarithmic dependence on density. Some of the difference between the Ostro et al. and Garvin et al. relationships (Fig. 2) may be due to the density range covered by the measurements. Garvin et al. used powders with bulk densities between 1 and 2.3 g cm^{-3}, while Ostro et al. sampled densities between 1.5 and 3.5 g cm^{-3}. These relationships are:

$$d = (R/R_{\text{Eros}})^{1/2}(3.75 \pm 0.1)\ \text{g/cm}^3 \quad \text{(Magri et al., 2001)},$$

$$d = 8.33R + (1.08 \pm 0.1)\ \text{g/cm}^3 \quad \text{(Ostro et al., 1985)},$$

$$d = \ln\left(\left(1 + R^{1/2}\right)/\left(1 - R^{1/2}\right)\right)(3.2 \pm 0.1)\ \text{g/cm}^3 \quad \text{(Garvin et al., 1985)}.$$

In the albedo regime of Phobos and Deimos, these density–reflectivity relationships are nearly linear. The Garvin et al. formula gives a near-surface density of 0.9 ± 0.2 g cm^{-3} for Deimos, the Ostro et al. formula gives 1.2 ± 0.2 g cm^{-3}, and the Magri et al. formula gives 1.1 ± 0.2 g cm^{-3}. There are similar differences for Phobos. In light of all the available information, we estimate an upper bound on Deimos' near-surface bulk density of 1.1 ± 0.3 g cm^{-3} and an upper bound on Phobos' near-surface bulk density of 1.6 ± 0.3 g cm^{-3}, where the indicated uncertainties are estimates of standard errors.

3. Implications

Phobos and Deimos have very similar optical and infrared spectra and inferred surface compositions, although Phobos has greater structural diversity (Thomas et al., 1999). Laboratory spectral analogs include lunar soils and heated, dehydrated, carbonaceous chondrites (Rivkin et al., 2002), both of which have grain densities about 2.7 g cm^{-3} (Britt and Consolmagno, 2003).

For an assumed grain density of 2.7 g cm^{-3}, our surface bulk density constraints imply mean near-surface porosities of at least $(40 \pm 10)\%$ on Phobos and $(60 \pm 10)\%$ on Deimos (porosity = 1 − bulk density/grain density). Neither porosity is implausible: for grains tens of microns in size, porosities near 70% are possible, either from electrostatic repulsion (e.g., Gold, 1962), or because of grain shape effects (e.g., very angular particles; Latham et al., 2002).

Why does Deimos have a higher surface porosity than Phobos, and why are the surface densities of Phobos and Deimos so low when compared to most other radar targets? Phobos and Deimos are in a unique dynamical environment: impact ejecta reaching escape velocity go into Mars orbit rather than escaping completely, as would be true for many small asteroids (Thomas et al., 1986; Veverka et al., 1986). This impact debris can then form very diffuse (100's of particles km^{-3}) dust bands around Mars (Soter, 1971; Krivov and Hamilton, 1997).

Particles smaller than about 30 μm are not stable on timescales of 100 yr in Phobos-like orbits: solar radiation pressure increases orbital eccentricities until the particles encounter Mars' atmosphere (Hamilton and Krivov, 1996). Similarly, particles smaller than ∼15 μm cannot remain in Deimos-like orbits around Mars. However, larger particles remain in well-defined bands for longer durations and can be re-accreted (Krivov and Hamilton, 1997). The velocity of dust-band particles during accretion is very low, comparable to the escape velocity, which is less than 20 m s^{-1} for Phobos (Davis et al., 1981; Veverka et al., 1986). Such low accretion velocities may lead to formation of high-porosity regolith, because particles settling relatively gently may be less likely to compress the material they land on.

Differences in regolith particle size can also contribute to the satellites' different near-surface densities. Phobos may have few particles smaller than

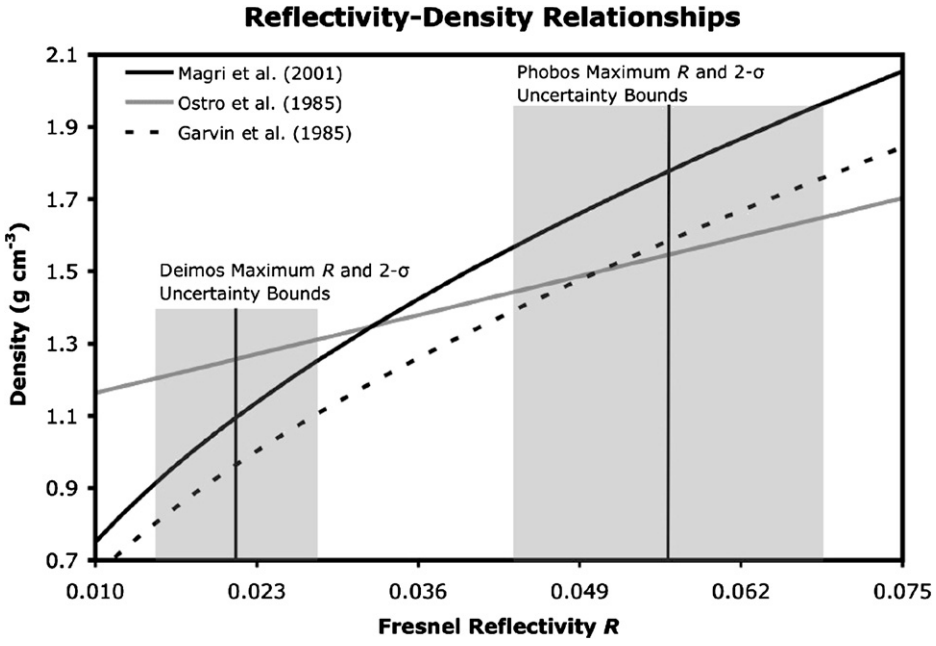

Fig. 2. Relationships between bulk density d and Fresnel reflection coefficient R, from Garvin et al. (1985), Ostro et al. (1985), and Magri et al. (2001). Upper bounds on R for Phobos and Deimos, with their 2-σ uncertainties, are denoted by gray shading.

30 μm, while Deimos can have particles down to ∼15 μm. 20 μm grains are small enough for electrostatic repulsion to possibly become significant enough to increase regolith porosity. Also, Deimos re-accretes any dust grains more efficiently than Phobos. Phobos' Hill radius (the approximate distance where tidal forces from Mars prevent any re-accretion) is 17 km, while Deimos' is 26 km. Deimos' lower mass is more than compensated by its greater distance from Mars. Deimos' 50% lower surface gravity may also contribute to higher regolith porosity.

In summary, Phobos and Deimos are both incredibly radar-dark. Deimos seems to have the lowest radar albedo ever observed for a Solar System object and probably is almost entirely covered by a very smooth, highly porous, dusty regolith likely composed largely of re-accreted ejecta. Phobos' regolith is low-density by asteroid standards, but is not as loosely packed as that of Deimos, perhaps due to Phobos having a combination of less efficient re-accretion, larger regolith particles, and/or higher surface gravity.

Acknowledgments

We thank P. Thomas for providing digital shape models of Phobos and Deimos. We thank the Arecibo technical staff for help with the observations. The Arecibo Observatory is part of the National Astronomy and Ionosphere Center, which is operated by Cornell University under a cooperative agreement with the National Science Foundation. C. Magri was partially supported by NSF Grant AST-0205975. J.F. Chandler and I.I. Shapiro were supported in part by NASA Grant NAGW-967. Part of this work was performed at the Jet Propulsion Laboratory, California Institute of Technology, under contract with the National Aeronautics and Space Administration (NASA). This material is based in part upon work supported by NASA under the Science Mission Directorate Research and Analysis Programs.

References

Benner, L.A.M., 2006. Summaries of asteroid radar properties. Available online at http://echo.jpl.nasa.gov/~lance/asteroid_radar_properties.html.

Britt, D.T., Consolmagno, G.J., 2003. Stony meteorite porosities and densities: A review of the data through 2001. Meteorit. Planet. Sci. 38, 1161–1180.

Davis, D.R., Housen, K.R., Greenberg, R., 1981. The unusual dynamical environment of Phobos and Deimos. Icarus 47, 220–233.

Garvin, J.B., Head, J.W., Pettengill, G.H., Zisk, S.H., 1985. Venus global radar reflectivity and correlations with elevation. J. Geophys. Res. B 90 (8), 6859–6871.

Gold, T., 1962. Processes on the lunar surface. In: Kopal, Z., Mikhailov, Z.K. (Eds.), The Moon. In: IAU Symposium, vol. 14. Lunar and Planetary Institute, Houston, TX, pp. 433–440.

Hamilton, D.P., Krivov, A.V., 1996. Circumplanetary dust dynamics: Effects of solar gravity, radiation pressure, planetary oblateness, and electromagnetism. Icarus 123, 503–523.

Jacobson, R.A., 1996. The orbital motion of the martian satellites: An application of artificial satellite theory, AA 96-1400. In: AAS/AIAA Spaceflight Mechanics Meeting, Austin, TX.

Jacobson, R.A., Rush, B., 2006. Ephemerides of the martian satellites—MAR063. JPL IOM 343R-06-004.

Krivov, A.V., Hamilton, D.P., 1997. Martian dust belts: Waiting for discovery. Icarus 128, 335–353.

Latham, J.P., Munjiza, A., Lu, Y., 2002. On the prediction of void porosity and packing of rock particulates. Powder Technol. 125, 10–27.

Magri, C., Consolmagno, G.J., Ostro, S.J., Benner, L.A.M., Beeney, B.R., 2001. Radar constraints on asteroid regolith properties using 433 Eros as ground truth. Meteorit. Planet. Sci. 36, 1697–1709.

Ostro, S.J., Campbell, D.B., Shapiro, I.I., 1985. Mainbelt asteroids: Dual-polarization radar observations. Science 229, 442–446.

Ostro, S.J., Jurgens, R.F., Yeomans, D.K., Standish, E.M., Greiner, W., 1989. Radar detection of Phobos. Science 243, 1584–1586.

Rivkin, A.S., Brown, R.H., Trilling, D.E., Bell, J.F., Plassmann, J.H., 2002. Near-infrared spectrophotometry of Phobos and Deimos. Icarus 156, 64–75.

Soter, S., 1971. The dust belts of Mars. CRSR Report No. 462, Cornell University.

Thomas, N., Britt, D.T., Herkenhoff, K.E., Murchie, S.L., Semenov, B., Keller, H.U., Smith, P.H., 1999. Observations of Phobos, Deimos, and bright stars with the imager for Mars Pathfinder. J. Geophys. Res. 104, 9055–9068.

Thomas, P., 1993. Gravity, tides, and topography on small satellites and asteroids. Icarus 105, 326–344.

Thomas, P., Veverka, J., Dermott, S., 1986. Small satellites. In: Burns, J.A., Matthews, M.S. (Eds.), Satellites. Univ. of Arizona Press, Tucson, pp. 802–835.

Veverka, J., Thomas, P., Johnson, T.V., Matson, D., Housen, K., 1986. The physical characteristics of satellite surfaces. In: Burns, J.A., Matthews, M.S. (Eds.), Satellites. Univ. of Arizona Press, Tucson, pp. 342–402.